

Supplement of Atmos. Chem. Phys., 18, 13655–13672, 2018  
<https://doi.org/10.5194/acp-18-13655-2018-supplement>  
© Author(s) 2018. This work is distributed under  
the Creative Commons Attribution 4.0 License.



Atmospheric  
Chemistry  
and Physics  
Open Access  
EGU

## *Supplement of*

The effects of intercontinental emission sources on European air pollution levels

**Jan Eiof Jonson et al.**

*Correspondence to:* Jan Eiof Jonson (j.e.jonson@met.no)

The copyright of individual parts of the supplement might differ from the CC BY 4.0 License.

In this supplementary material we include additional tables and figures not included in the paper. Table 1 provides basic information and references to the HTAP2 models included in this study. The models are a subset of the HTAP2 models listed and described in Stjern et al. (2016). Since then additional model result have also been provided for the GFDL\_AM3 model (uploaded to the HTAP2 database in raw format), raising the number of models to 8. The GFDL\_AM3 simulations for HTAP2 include interactive stratospheric and tropospheric aerosols and chemistry at approximately 100x100 km<sup>2</sup> resolution nudged to NCEP winds using a pressure-dependent nudging technique (Lin et al., 2012). Analysis of long-term observations indicate that GFDL-AM3 captures the impacts of rising Asian emissions and intercontinental transport on free tropospheric and surface ozone trends over North America and Europe during the past few decades (Lin et al., 2015, Lin et al., 2017).

In addition we include comparisons of model results with surface and sonde measurements. In the paper the main focus is on Europe, and this is also reflected in the selection of measurement sites.

Below we also compare model results to measurements at mountain sites. These results should be interpreted with caution as the height of the measurement sites will be well above the model surface for all models. Elevation will also differ between the models depending on vertical and horizontal resolution and model topography.

## References

- Henze, D. K., Hakami, A., and Seinfeld, J. H.: Development of the adjoint of GEOS-Chem, *Atmospheric Chemistry and Physics*, 7, 2413–2433, doi: 10.5194/acp-7-2413-2007, URL <https://www.atmos-chem-phys.net/7/2413/2007/>, 2007.
- Huijnen, V., Flemming, J., Chabrillat, S., Errera, Q., Christophe, Y., Blechschmidt, A.-M., Richter, A., and Eskes, H.: C-IFS-CB05-BASCOE: stratospheric chemistry in the Integrated Forecasting System of ECMWF, *Geoscientific Model Development*, 9, 3071–3091, doi:10.5194/gmd-9-3071-2016, URL <https://www.geosci-model-dev.net/9/3071/2016/>, 2016.
- Lin, M., Fiore, A. M., Horowitz, L. W., Cooper, O. R., Naik, V., Holloway, J., Johnson, B. J., Middlebrook, A. M., Oltmans, S. J., Pollack, I. B., Ryerson, T. B., Warner, J. X., Wiedinmyer, C., Wilson, J., and Wyman, B.: Transport of Asian ozone pollution into surface air over the western United States in spring, *Journal of Geophysical Research: Atmospheres*, 117, 0148–0227, doi:10.1029/2011JD016961, URL <https://agupubs.onlinelibrary.wiley.com/doi/abs/10.1029/2011JD016961>, 2012.
- Lin, M., Horowitz, L. W., Cooper, O. R., Tarasick, D., Conley, S., Iraci, L. T., Johnson, B., Leblanc, T., Petropavlovskikh, I., and Yates, E. L.: Revisiting the evidence of increasing springtime ozone mixing ratios in the free troposphere over western North America, *Geophysical Research Letters*, 42, 8719–8728, doi:10.1002/2015GL065311, URL <http://dx.doi.org/10.1002/2015GL065311>, 2015GL065311, 2015.
- Lin, M., Horowitz, L. W., Payton, R., Fiore, A. M., and Tonnesen, G.: US surface ozone trends and extremes from 1980 to 2014: quantifying the roles of rising

- Asian emissions, domestic controls, wildfires, and climate, *Atmospheric Chemistry and Physics*, 17, 2943–2970, doi:10.5194/acp-17-2943-2017, URL <https://www.atmos-chem-phys.net/17/2943/2017/>, 2017.
- Simpson, D., Benedictow, A., Berge, H., Bergström, R., Emberson, L., Fagerli, H., Flechard, C., Hayman, G., Gauss, M., Jonson, J., Jenkin, M., Nyíri, A., Richter, C., Semeena, V., Tsyro, S., Tuovinen, J.-P., Valdebenito, A., and Wind, P.: The EMEP MSC-W chemical transport model technical description, *Atmos. Chem. Phys.*, 12, 7825–7865, doi:10.5194/acp-12-7825-2012, 2012.
- Søvde, O. A., Prather, M. J., Isaksen, I. S. A., Berntsen, T. K., Stordal, F., Zhu, X., Holmes, C. D., and Hsu, J.: The chemical transport model Oslo CTM3, *Geoscientific Model Development*, 5, 1441–1469, doi:10.5194/gmd-5-1441-2012, URL <https://www.geosci-model-dev.net/5/1441/2012/>, 2012.
- Stjern, C. W., Samset, B. H., Myhre, G., Bian, H., Chin, M., Davila, Y., Dentener, F., Emmons, L., Flemming, J., Haslerud, A. S., Henze, D., Jonson, J. E., Kucsera, T., Lund, M. T., Schulz, M., Sudo, K., Takemura, T., and Tilmes, S.: Global and regional radiative forcing from 20% reductions in BC, OC and SO<sub>4</sub> – an HTAP2 multi-model study, *Atmospheric Chemistry and Physics*, 16, 13579–13599, doi:10.5194/acp-16-13579-2016, URL <http://www.atmos-chem-phys.net/16/13579/2016/>, 2016.
- Sudo, K., Takahashi, M., Kurokawa, J.-I., and Akimoto, H.: CHASER: A global chemical model of the troposphere 1. Model description, *J. Geophys. Res.*, 107, doi:10.1029/2001JD001113., 2002.
- Tilmes, S., Lamarque, J.-F., Emmons, L. K., Kinnison, D. E., Marsh, D., Garcia, R. R., Smith, A. K., Neely, R. R., Conley, A., Vitt, F., Val Martin, M., Tanimoto, H., Simpson, I., Blake, D. R., and Blake, N.: Representation of the Community Earth System Model (CESM1) CAM4-chem within the Chemistry-Climate Model Initiative (CCMI), *Geoscientific Model Development*, 9, 1853–1890, doi:10.5194/gmd-9-1853-2016, URL <https://www.geosci-model-dev.net/9/1853/2016/>, 2016.

Table 1: Models providing vertical profiles of ozone for the TF HTAP intercomparison. Documentation of the models can be found at <http://www.htap.org/> under the heading: Model Descriptions. Only the 7 first models (in bold) provided vertical profiles for the SR20% scenarios.

Model	Resolution (lat long)	layers	Meteorology	Institution	Main reference
<b>EMEP rv48</b>	0.5° x 0.5°	20 <sup>1</sup>	ECMWF (IFS)	Met Norway, Oslo, Norway	Simpson et al. (2012)
<b>IFS v2</b>	0.7° x 0.7°	54	Relaxed to ERA interim	ECMWF, UK	Huijnen et al. (2016)
<b>OsloCTM3_v2</b>	2.8° x 2.8°	60	ECMWF (IFS)	Univ. of Oslo, Norway	Søvde et al. (2012)
<b>CAMchem</b>	1.9° x 2.5°	56	GEOOS5 v5.2	NCAR, CO, USA	Tilmes et al. (2016)
<b>CHASER-t42</b>	2.8° x 2.8°	32	Mainly ERA interim	Univ. Nagoya, Japan	Sudo et al. (2002)
<b>CHASER-t106</b>	1.1° x 1.1°	32	Mainly ERA interim	Univ. Nagoya, Japan	Sudo et al. (2002)
<b>GEOSCHEMADJ.</b>	2.0° x 2.5°	47 <sup>3</sup>	GEOOS5 (MERRA)	Univ. Colorado, Boulder, CO, USA	Henze et al. (2007)
GFDL AM3	1.25° x 1.0°	48	NCEP <sup>2</sup>	Univ. Colorado, Boulder, CO, USA	Lin et al. (2012,2015,2017)

<sup>1</sup> O<sub>3</sub> read in from ECMWF IFS model every 3 hours at upper boundary

<sup>2</sup> The GFDL-AM3 simulations for HTAP2 include interactive stratospheric aerosols and chemistry nudged to NCEP winds using a pressure-dependent nudging technique (Lin et al., 2012). Analysis of long-term observations indicate that GFDL-AM3 captures the impacts of rising Asian emissions on free tropospheric and surface ozone trends over North America over the past few decades (Lin et al., 2015; Lin et al., 2017).

<sup>3</sup> This model version only simulates O<sub>3</sub> in the troposphere. Stratospheric O<sub>3</sub> levels based on boundary conditions.

### CO Mountain sites

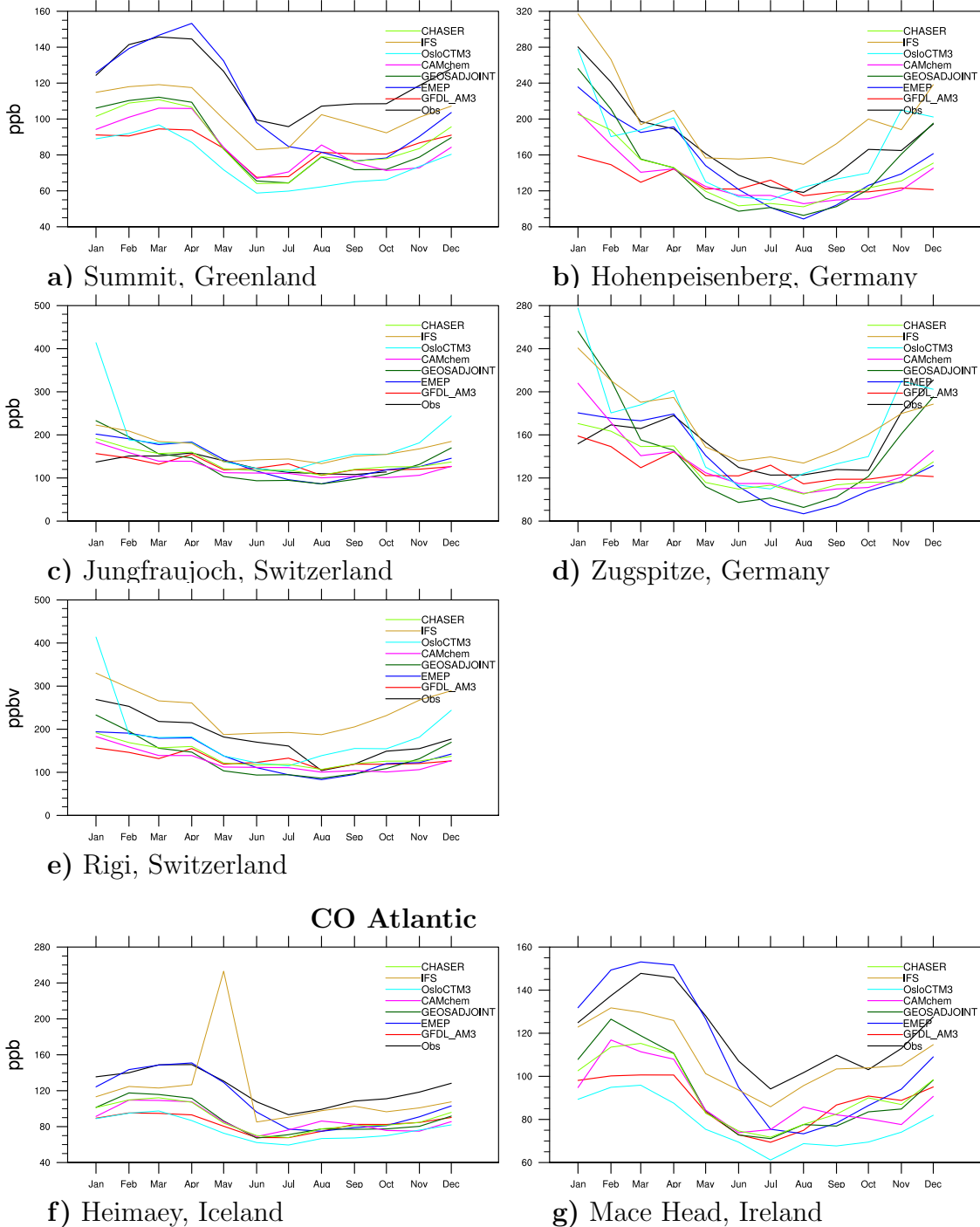


Figure S1: Models versus measurements of CO in ppb at mountain and Atlantic sites. Annual average concentrations and correlations are tabulated in the paper.

## CO Western and central Europe

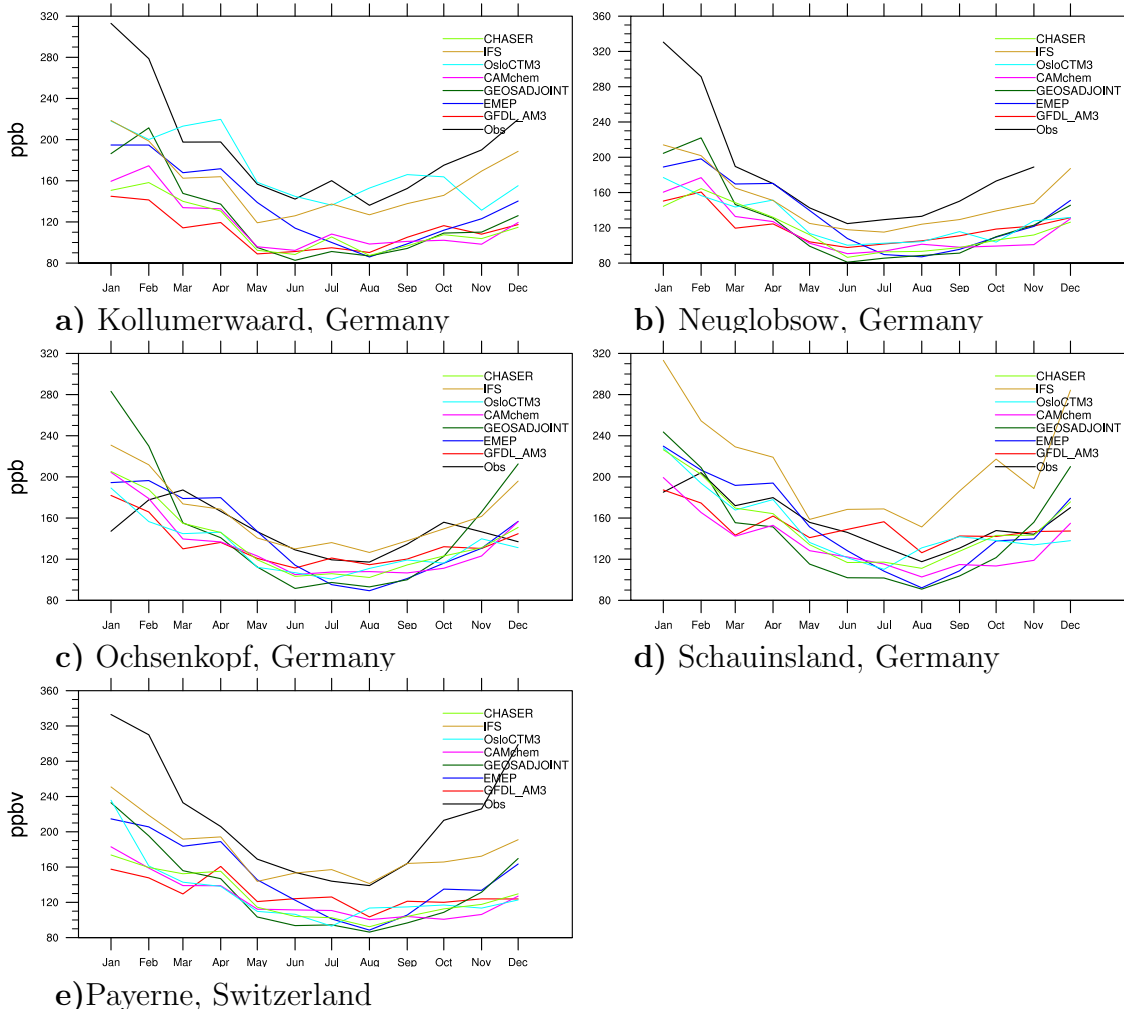


Figure S2: Western and central Europe models versus measurements of CO in ppb.  
Annual average concentrations and correlations are tabulated in the paper.

### CO Southern and eastern Europe

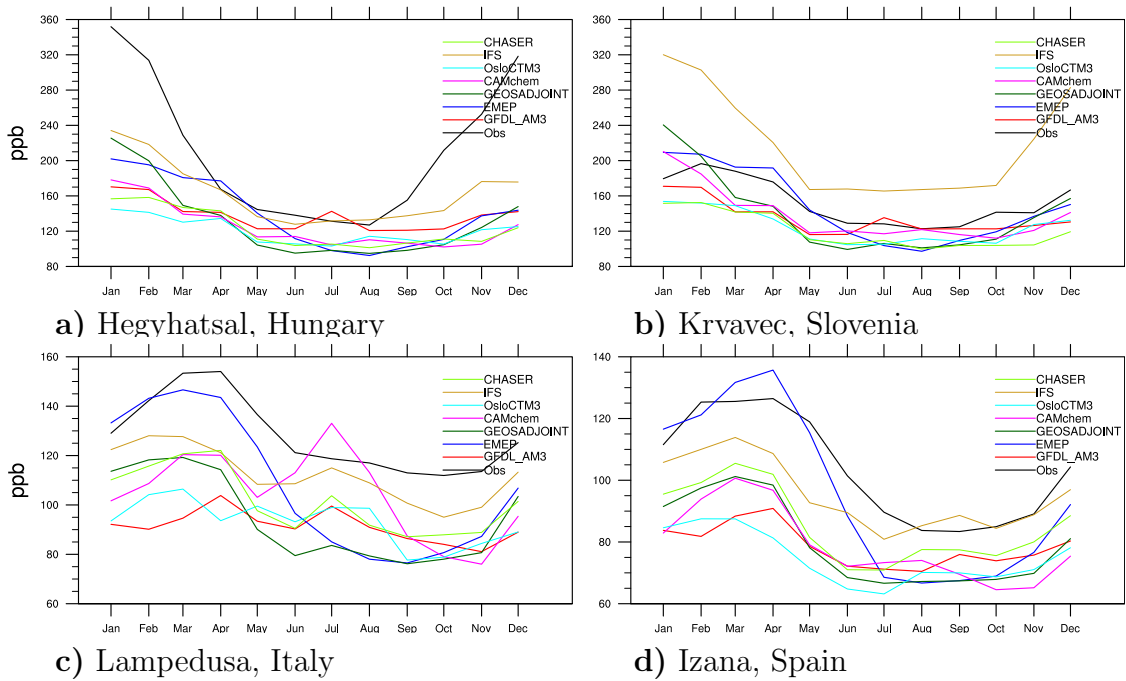


Figure S3: Eastern and southern Europe and Models versus measurements of CO in ppb. Annual average concentrations and correlations are tabulated in the paper.

### Ozone Western and northern Europe

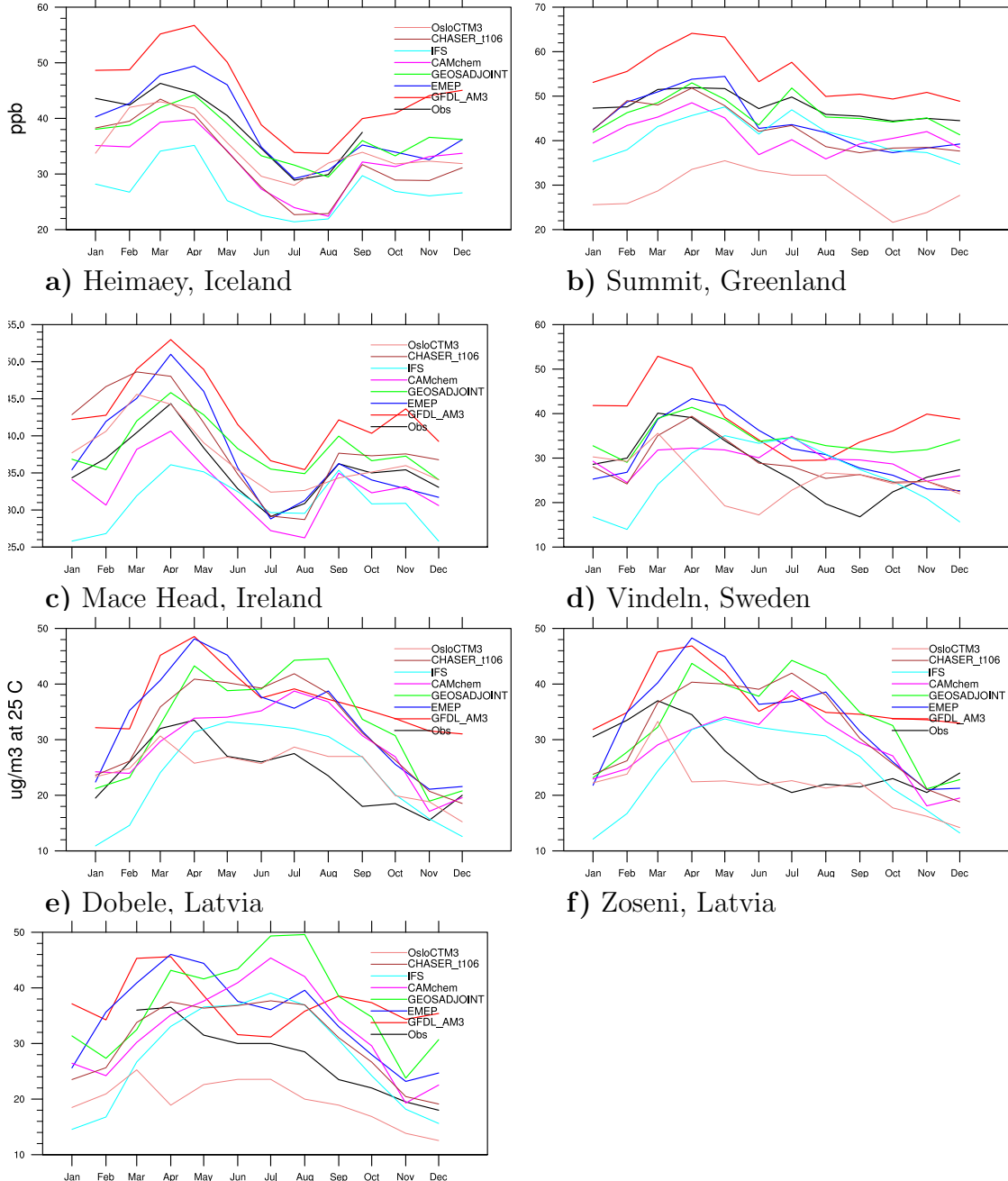


Figure S4: Western and northern Europe models versus measurements of ozone in ppb. Annual average concentrations and correlations are tabulated in the paper.

### Ozone Central Europe

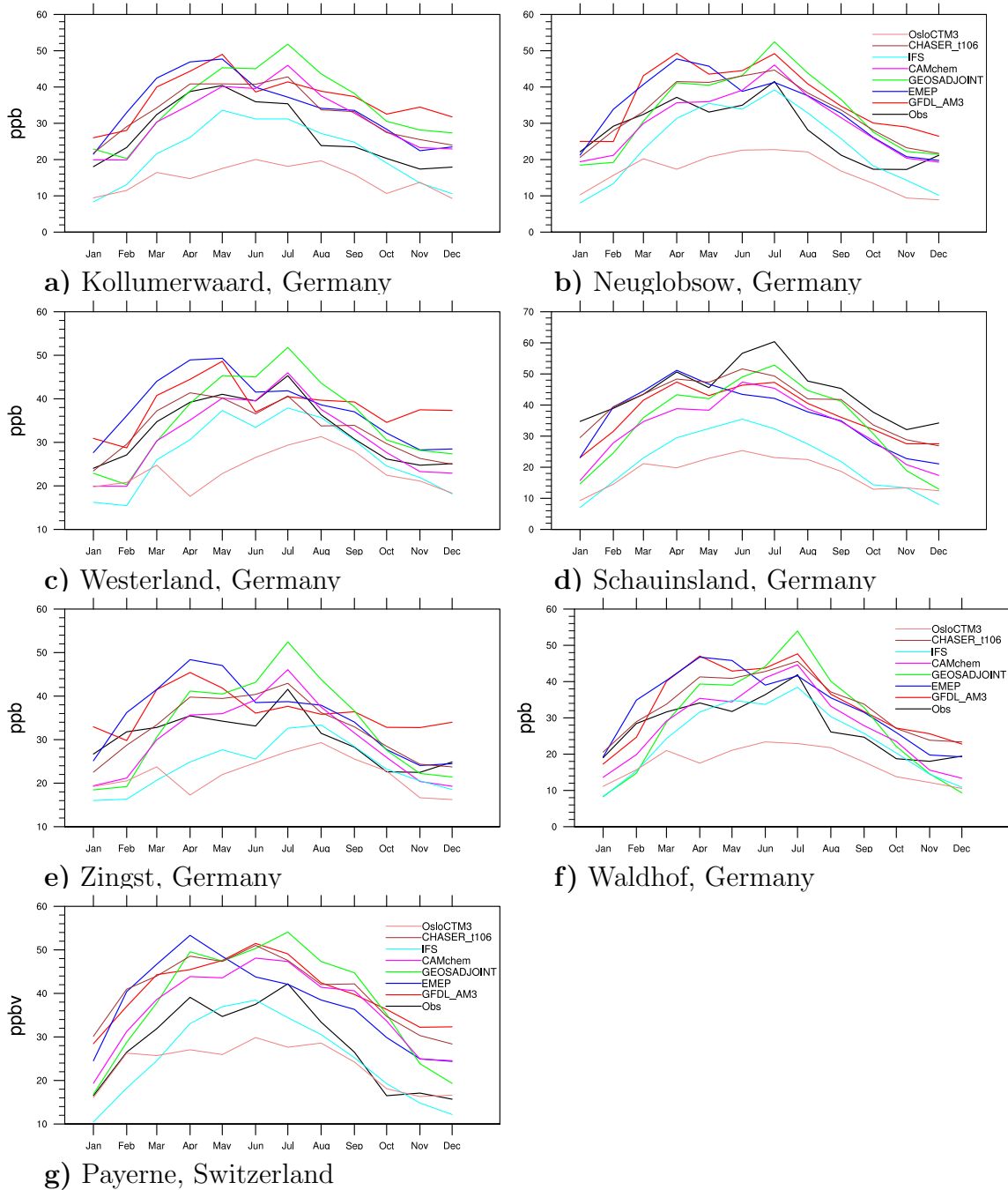


Figure S5: Central Europe models versus measurements of ozone in ppb. Annual average concentrations and correlations are tabulated in the paper.

### Ozone Eastern Europe

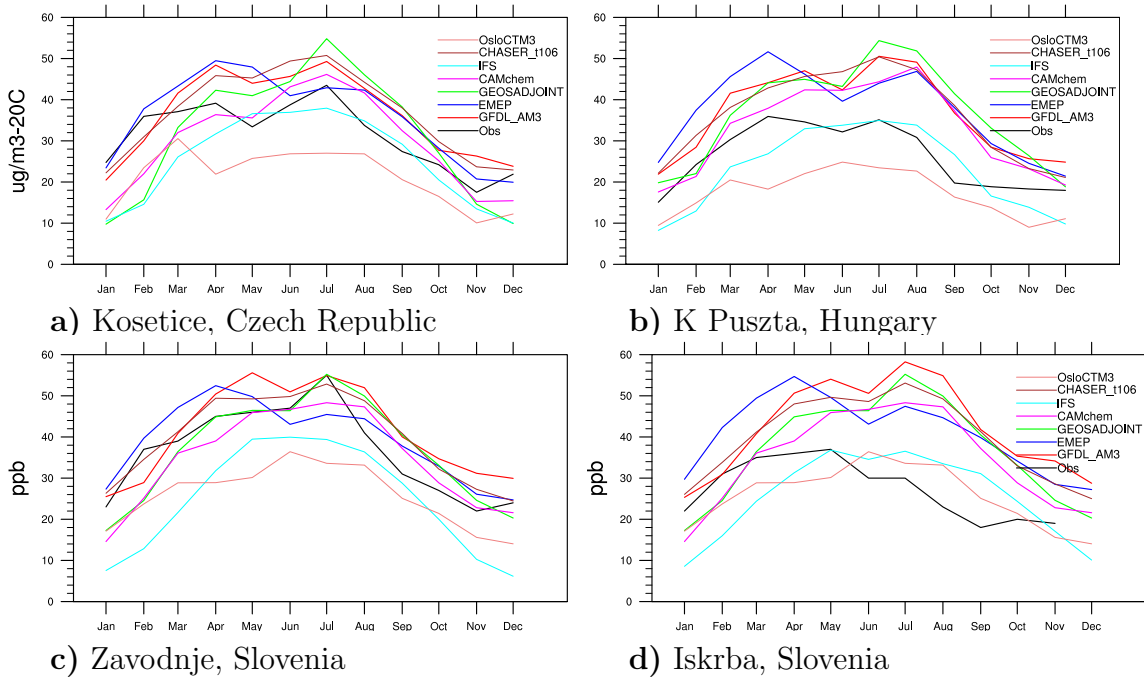
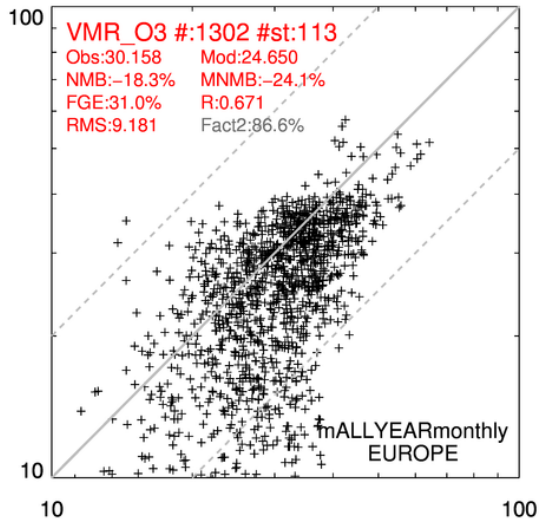
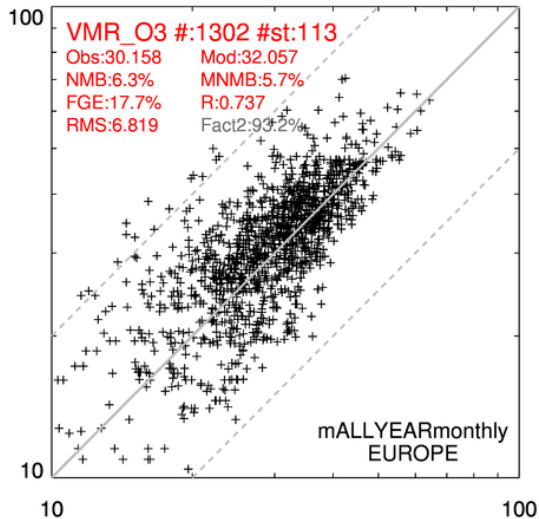


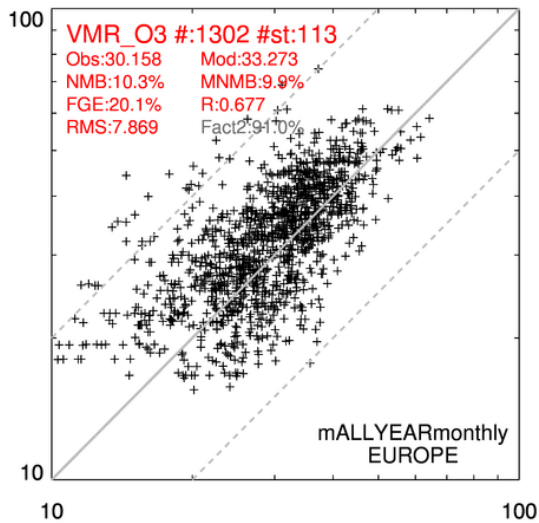
Figure S6: Eastern Europe models versus measurements of ozone in ppb. Annual average concentrations and correlations are tabulated in the paper.



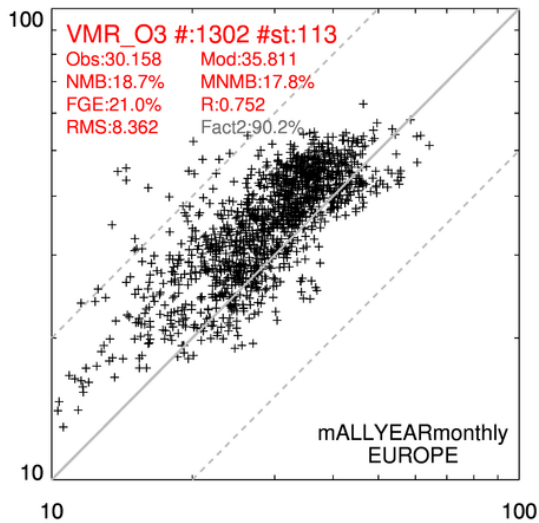
a) IFS2



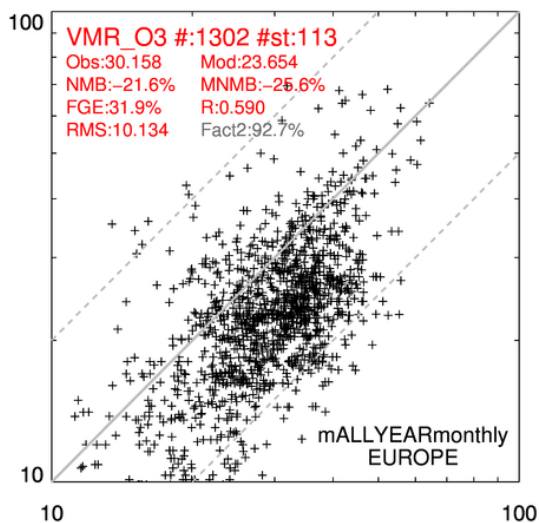
b) CAMchem



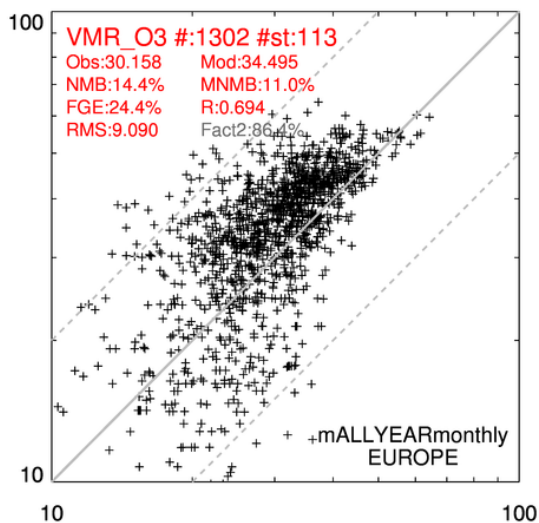
c) CHASER\_rel



d) EMEP



e) OsloCTM3



f) GEOS-Chem

Figure S7: O<sub>3</sub> annual scatter plots in ppb processed by use of the AEROCOM tool, see [http://aerocom.met.no/cgi-bin/aerocom/surfobs\\_annualrs.pl?PROJECT=HTAP&MODELLIST=HTAP-phaseII](http://aerocom.met.no/cgi-bin/aerocom/surfobs_annualrs.pl?PROJECT=HTAP&MODELLIST=HTAP-phaseII). Measurement data originally downloaded from EBAS, <http://ebas.nilu.no/Default.aspx>. Measured: x-axis, modelled: y-axis.

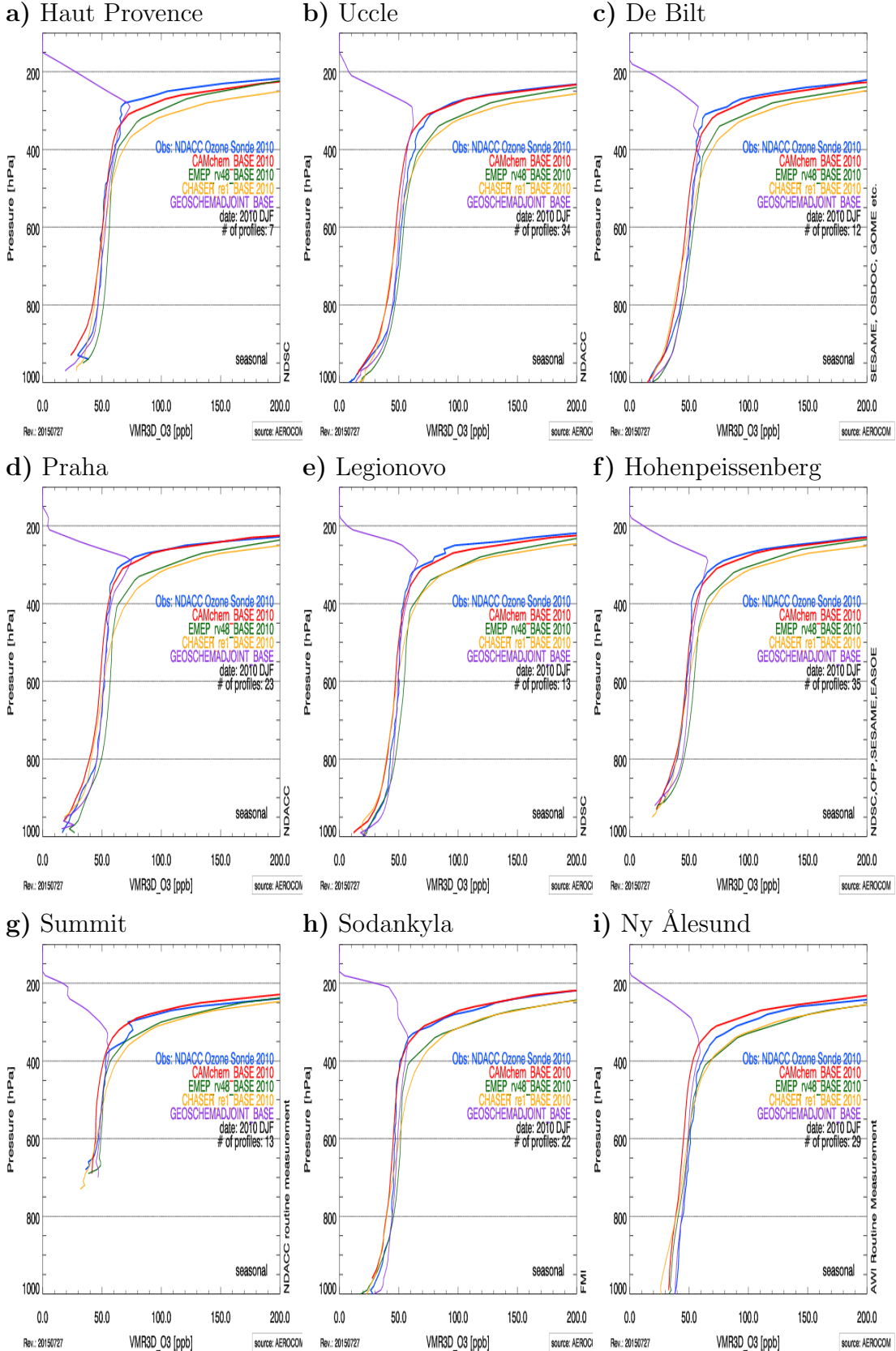


Figure S8: Model calculated O<sub>3</sub> vertical profiles versus ozone sondes averaged for the winter months December, January and February. The Model calculated vertical ozone are calculated based on the approximate same dates and times as the sonde measurements. The number of sonde measurements included for each site is listed in the panels.

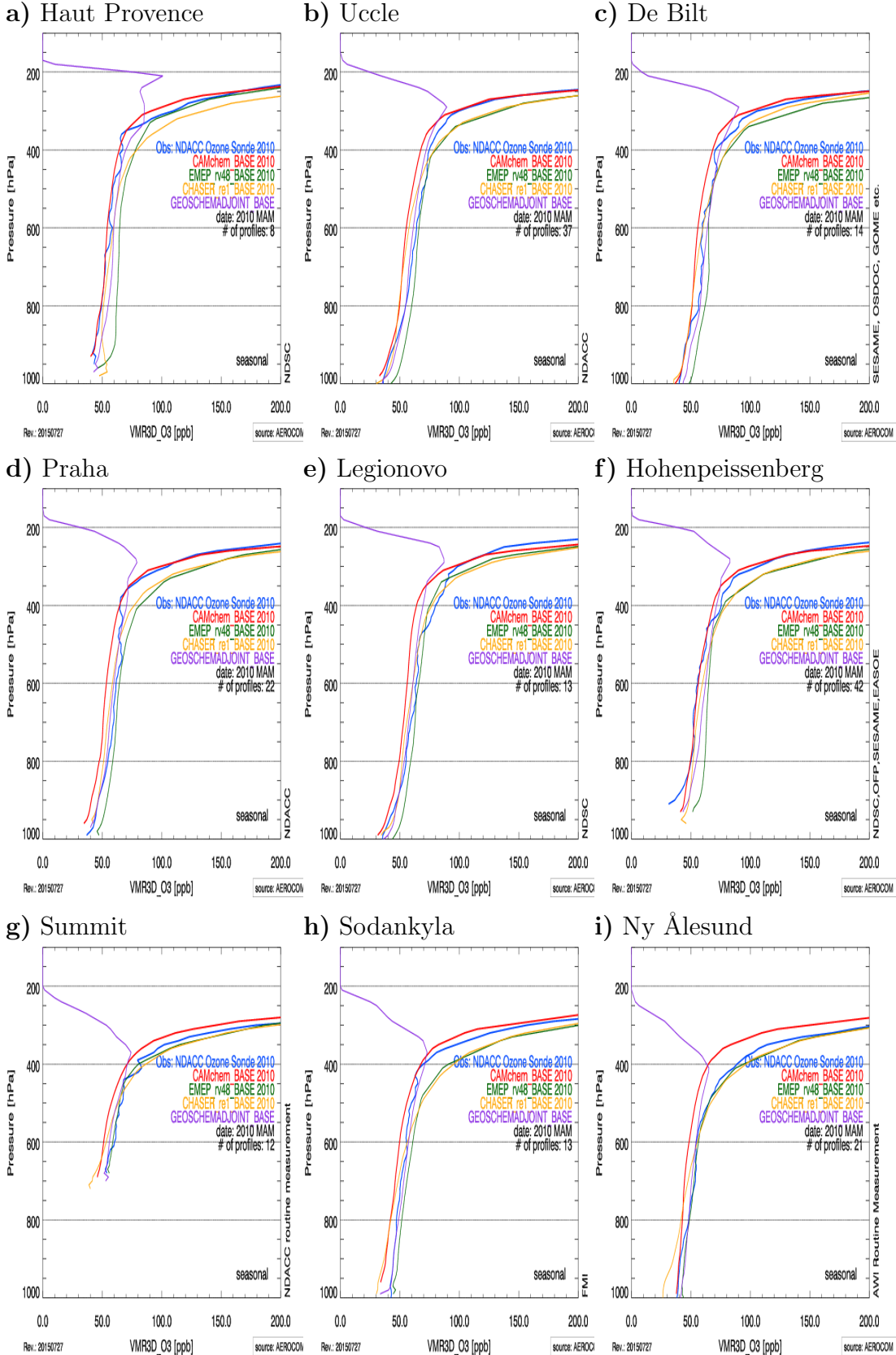


Figure S9: Model calculated O<sub>3</sub> vertical profiles versus ozone sondes averaged for the spring months March, April and May. The Model calculated vertical ozone are calculated based on the approximate same dates and times as the sonde measurements. The number of sonde measurements included for each site is listed in the panels.

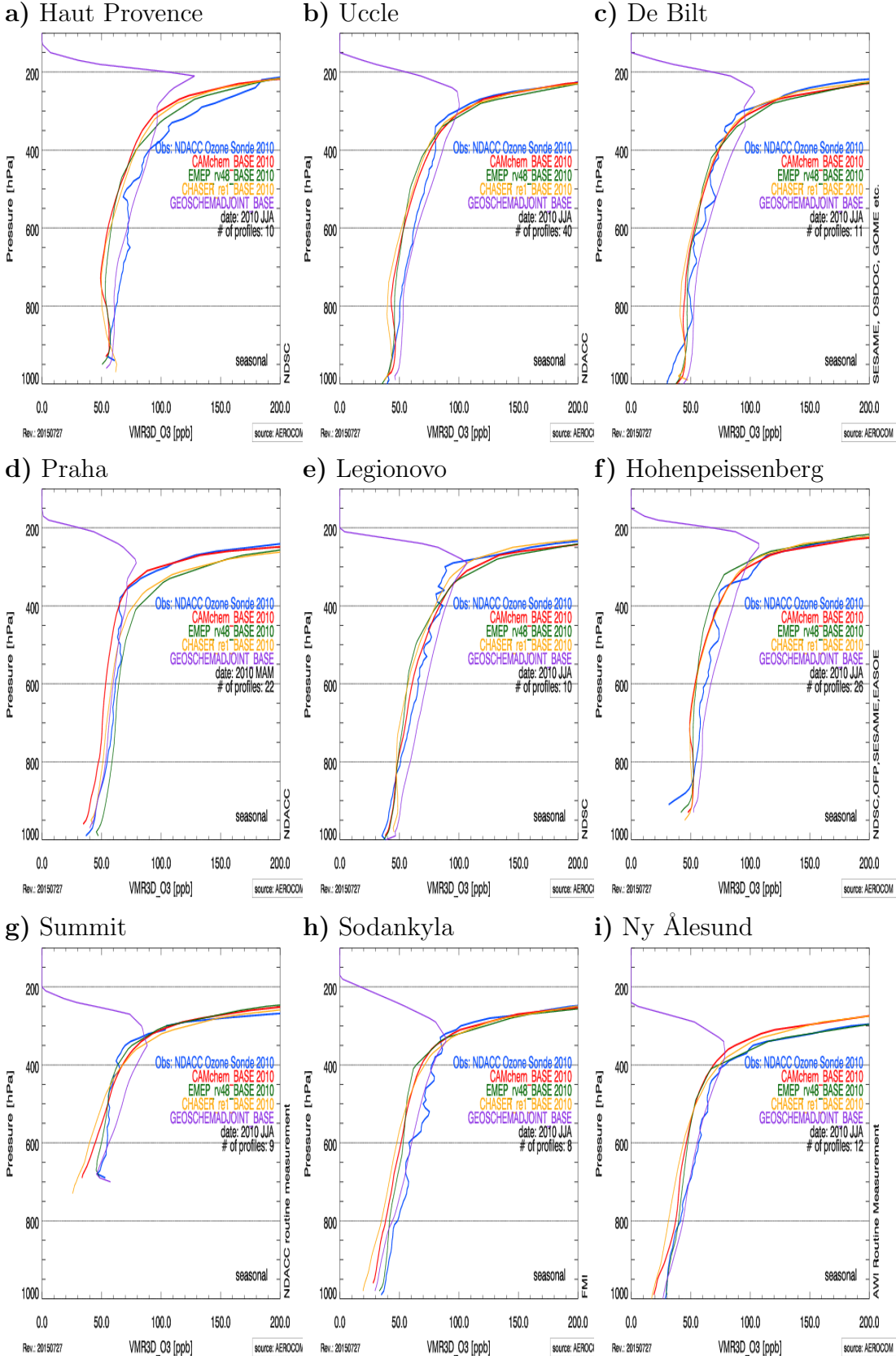


Figure S10: Model calculated O<sub>3</sub> vertical profiles versus ozone sondes averaged for the summer months June, July and August. The Model calculated vertical ozone are calculated based on the approximate same dates and times as the sonde measurements. The number of sonde measurements included for each site is listed in the panels.

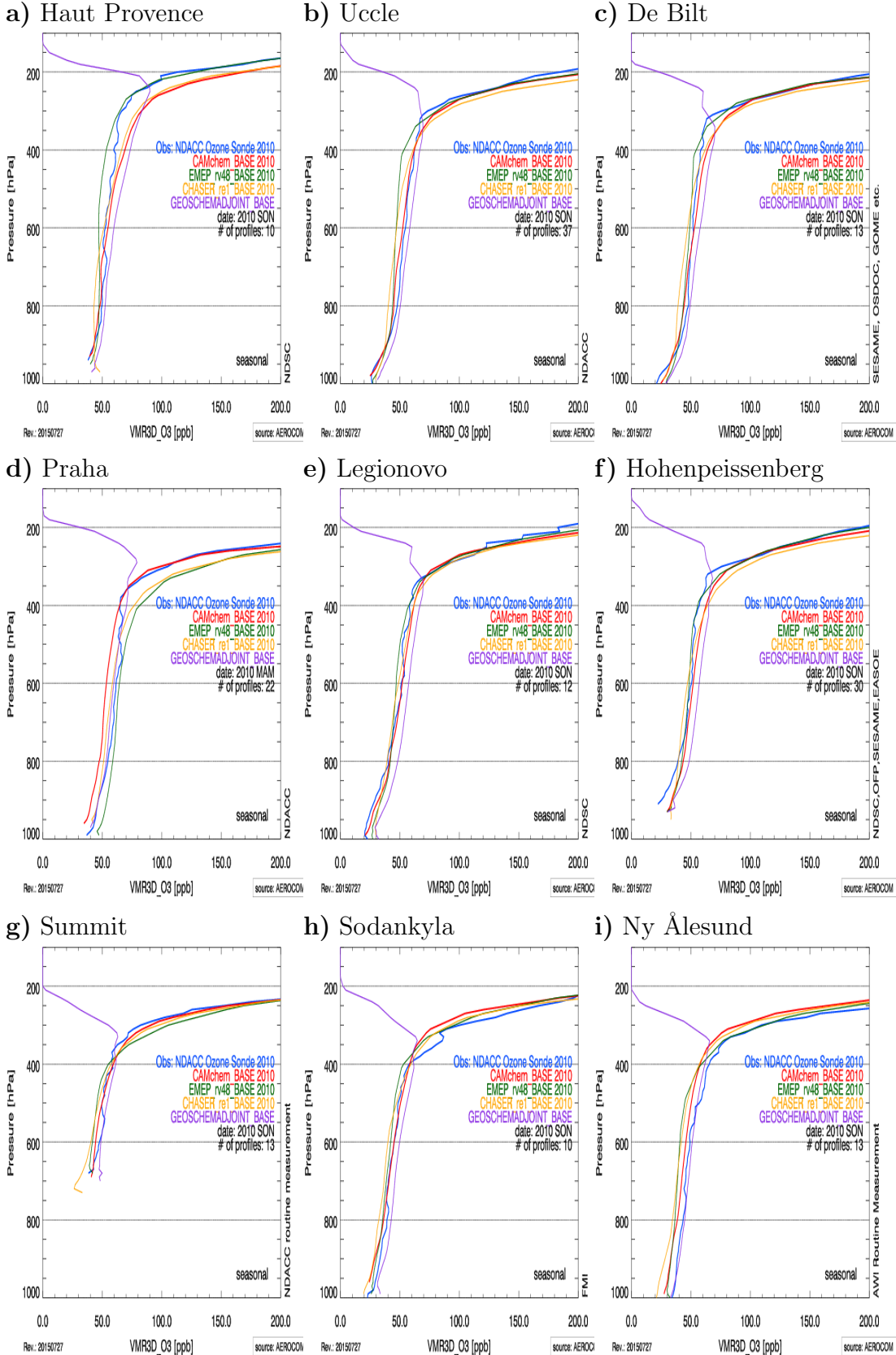


Figure S11: Model calculated O<sub>3</sub> vertical profiles versus ozone sondes averaged for the autumn months September, October and November. The Model calculated vertical ozone are calculated based on the approximate same dates and times as the sonde measurements. The number of sonde measurements included for each site is listed in the panels.

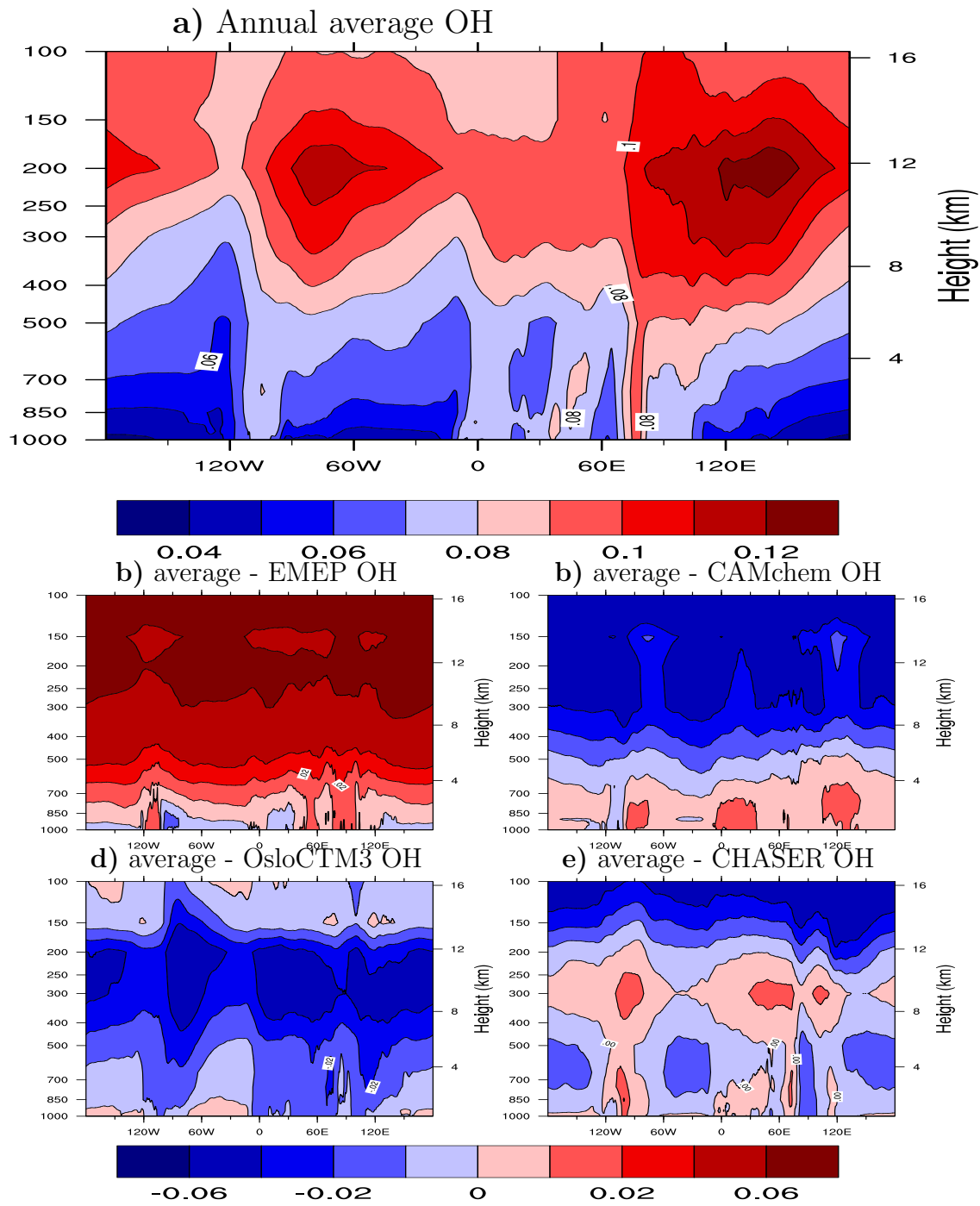


Figure S12: Top, annually averaged OH in ppt between 30 and 60 degrees north for the four models: EMEP\_rv4,8, CAMCHEM, OsloCTM3, CHASER\_re1. b,c,d,e are difference between average OH and the same four models.